CNS Neuroscience & Therapeutics

ORIGINAL ARTICLE

CNS Neuroscience & Therapeutics

NF-κB Signaling is Involved in the Effects of Intranasally Engrafted Human Neural Stem Cells on Neurofunctional Improvements in Neonatal Rat Hypoxic–Ischemic Encephalopathy

Gang Ji,[1] Ming Liu,[1] Xiong-Fei Zhao,[2] Xiao-Yan Liu,[1] Qi-Lin Guo,[1] Zhu-Fei Guan,[3] Hou-Guang Zhou[3] & Jing-Chun Guo[1]

1 State Key Laboratory of Medical Neurobiology, School of Basic Medical Sciences, Shanghai Medical College, Fudan University, Shanghai, China
2 Shanghai Angecon Biotechnology Co., Ltd., Shanghai, China
3 Department of Geriatric Neurology, Huashan Hospital, Fudan University, Shanghai, China

Keywords
Hypoxia–ischemia; Neurobehavioral recovery; Neuroimmunomodulation; NF-κB; Stem cell.

Correspondence
J.-C. Guo, Ph.D., State Key Laboratory of Medical Neurobiology, Shanghai Medical College, Fudan University, 131 DongAn Rd, Shanghai 200032, China.
Tel.: +86-21-54237231;
Fax: +86-21-64174579;
E-mail: jingchunguo@shmu.edu.cn
and
H.-G. Zhou, M.D, Ph.D., Department of Geriatrics Neurology, Huashan Hospital, Fudan University, 12 Middle WuLuMuQi Rd, Shanghai 200040, China.
Tel.: +86-21-52887292;
Fax: +86-21-52887315;
E-mail: zhg7376@163.com
Received 27 March 2015; revision 9 July 2015; accepted 10 July 2015

SUMMARY

Aim: Hypoxic–ischemic encephalopathy (HIE) is a common neurological disease in infants with persistent neurobehavioral impairments. Studies found that neural stem cell (NSC) therapy benefits HIE rats; however, the mechanisms underlying are still unclear. The current study investigated the efficacy and molecular events of human embryonic neural stem cells (hNSCs) in neonatal hypoxic–ischemic (HI) rats. **Methods:** PKH-26-labeled hNSCs were intranasally delivered to P7 Sprague Dawley rats 24 h after HI. Neurobehavioral tests were performed at the indicated time after delivery: righting reflex and gait testing at D1, 3, 5, and 7; grid walking at D7 and 14; social choice test (SCT) at D28; and Morris water maze from D35 to 40. Protein expression was determined by Western blot analysis. Brain damage was assessed by cresyl violet staining and MBP staining. hNSC distribution and differentiation were observed by *in vivo* bioluminescence imaging and immunofluorescence staining. **Results:** (1) hNSCs migrated extensively into brain areas within 24 h after the delivery, survived even at D42 with the majority in ipsi-hemisphere, and could be co-labeled with NeuN or GFAP. (2) hNSCs reduced the upregulation in cytosolic IL-1β, p-IκBα, and NF-κB p65 levels, whereas enhanced nuclear p65 expression in HI rats at D3 after the delivery. (3) hNSCs decreased HI-induced brain tissue loss and white matter injury at D42 after the delivery. (4) hNSCs improved neurological outcomes in HI rats in the tests of righting reflex (within 3 days), gait (D5), grid (D7), SCT (D28), and water maze (D42). **Conclusion:** Intranasal delivery of hNSCs could prevent HI-induced brain injury and improve neurobehavioral outcomes in neonatal HI rats, which is possibly related to the modulation of NF-κB signaling.

doi: 10.1111/cns.12441

Introduction

Perinatal hypoxic–ischemic encephalopathy (HIE) is one of the major causes of neonatal sensorimotor disabilities, cognitive deficits, and learning and memory disorders [1–3]. Although prolonged moderate cerebral hypothermia has been reported to improve the outcome for HIE children, it still cannot eliminate the combined risk of disability and death [4]. Neural stem cells (NSCs) possess multipotential and self-renewal abilities and are well known with low immunogenicity [5], thus becoming a candidate for HIE therapy. However, studies focusing on the efficacy and molecular events of NSCs in HIE are still limited.

Cerebral hypoxia–ischemia (HI) injury initiates biochemical cascade reactions, such as excitatory toxicity, neuroinflammation, and reactive oxygen species production, which ultimately lead to neuronal death and white matter injury [6]. Previous studies have demonstrated that transcriptional factor NF-κB controls transcription of series of downstream genes and plays important roles in inflammation, cell survival, and apoptosis [7–9]. More interestingly, NF-κB inhibition is reported to impair the long-term memory formation and reconsolidation [10]. These results indicate that NF-κB signaling is possibly involved in critical cellular and systemic events in the process of HI-induced brain damage and therapeutic interventions. Therefore, we asked whether NF-κB signaling participates in the protective efficacy of NSCs against HI injury.

In this study, we utilized nasal administration of human embryonic neural stem cells (hNSCs) on neonatal rat HI model and evaluated protective efficacy of hNSCs on HI injury. Our results found

for the first time that hNSCs could promote NF-κB translocation in neonatal HI rats. Additionally, we found that hNSCs could inhibit the IL-1β expression, reduce brain tissue loss and white matter injury, ameliorate sensorimotor dysfunction, and further improve long-term learning, memory, and cognitive functions after HI.

Materials and Methods

hNSC Culture and PKH-26 Labeling

Well-characterized human embryonic NSCs were obtained from Shanghai Angecon Biotechnology Co., Ltd. (Shanghai, China). Cells were seeded and cultured in growth medium DMEM/F12 (1:1) supplement with 1% B27, 1% NAC, 1% L-glutamine, 1% sodium pyruvate, 20 ng/mL bFGF, 20 ng/mL EGF, and 10 ng/mL leukemia inhibitory factor (all from Invitrogen, Carlsbad, CA, USA). For cell labeling, 2×10^7 single cells were placed in suspension and washed once using saline. After being centrifuged ($400 \times g$) for 5 min, cells were carefully resuspended. PKH-26 ethanolic dye solution (Sigma, St. Louis, MO, USA) was added as the method described [11]. After centrifugation, 3×10^5 cells were resuspended in 6 μL saline for intranasal delivery.

Neonatal HI Rat Model and Intranasal Delivery of hNSCs

All the animal experiments were approved by the Institutional Animal Care and Use Committee of Fudan University. All efforts were made to minimize the suffering of animals. Postnatal day 7 Sprague Dawley rats (Shanghai Super-B&K laboratory animal Corp. Ltd., Shanghai, China) were used to establish HI model according to the methods described previously [12] with slight modifications. Briefly, the left common carotid artery of rats was exposed, isolated, and cut using electrocoagulation knife under anesthesia with diethyl ether. The duration of anesthesia and surgery were controlled within 5 min. After a 1.5-h recovery period, pups were exposed to hypoxia (7.8% O_2, 92.2% N_2) for 120 min at 37°C and then returned to their dam for the indicated time. Rats underwent the same surgery without common carotid cutting and the following hypoxia were served as sham-operation animals. For intranasal delivery, a total volume of 6 μL cell suspension solution (3×10^5 cells) or vehicle (saline) was applied at 24 h after HI, in alternating 3 μL portions for each nostril according to the method described previously [13]. For animal grouping, before surgery, all the pups were randomly divided into four groups: sham + saline, sham + hNSCs, HI + saline, and HI + hNSCs. The total number of neonatal rats in this study was 138.

Fluorescence Imaging of PKH-26-Labeled Cells

At 3 h after hNSC application, *in vivo* bioluminescence imaging was acquired on the head of pups using IVIS Lumina XR Imaging system (PerkinElmer, Waltham, MA, USA). Total fluorescence efficiency was analyzed using the software IVIS Lumina II Living Image 4.3 (PerkinElmer) to reflect the migration and distribution of hNSCs in the brain. At 24 h after the application, animals were transcardially perfused with 4% paraformaldehyde in phosphate-buffered saline under diethyl ether anesthesia, and their brains were removed. Postfixation and cryoprotection was then performed as the method described [1]. After that, coronal sections (30 μm) were cut using a microtome (Leica, Wetzlar, Germany) and screened for observation of PKH-26-positive cells under fluorescence microscopy (Olympus, Tokyo, Japan).

Protein Preparation

At 72 h after hNSC application, cytoplasmic and nuclear protein extracts from fresh ipsilateral brain tissues were prepared. Briefly, tissues (150–200 mg) were cut into small pieces in chilled buffer A (20 mM Hepes, 1 mM $MgCl_2$, 0.5 mM EDTA, 1 mM EGTA, 1 mM DTT, 0.5 mM PMSF, measured pH 7.9, 0.5% Triton X-100, plus inhibitors) and ruptured by homogenizer on ice. Crude nuclei pellets were collected after centrifugation at $1000 \times g$ for 5 min at 4°C. Centrifugation of supernatants at $161{,}000 \times g$ for 8 min at 4°C gave pellets as membrane/cytoskeleton and the supernatant as cytosolic fraction. Crude nuclei pellets were then washed twice with buffer A, spin at $1000 \times g$ for 5 min at 4°C, and suspended with chilled buffer B (20 mM Hepes, 300 mM NaCl, 1.5 mM $MgCl_2$, 0.2 mM EDTA, 1 mM EGTA, 1 mM DTT, 0.5 mM PMSF, measured pH 7.9, 1% SDS, and 10% glycerol, plus inhibitors). After vortex, ultrasonic disruption and centrifugation at $161{,}000 \times g$ for 5 min at 4°C, the supernatant was collected as nuclear protein extracts. Protein contents of each fraction were determined by bicinchoninic acid assay (Beyotime Biotechnology, Beijing, China).

Western Blot

Protein samples (15 μg/lane) from different groups were electrophoresed on 10% SDS–polyacrylamide gel and transferred to the polyvinyl difluoride membrane (Bio-Rad, Hercules, CA, USA) as the method described [14]. Peroxidase activity was visualized with an enhanced chemiluminescence substrate system (ECL; Santa Cruz Biotechnology, Santa Cruz, CA, USA). Protein band intensities were corrected with β-actin or histone H3, and quantified using Quantity One (Bio-Rad). The following primary and secondary antibodies were used: mouse anti-IκB-α (phospho S32 + S36, 1:500; Abcam), rabbit anti-NF-κB p65 (1:500; Abcam, Cambridge, UK), rabbit antihistone H3 (1:500; ABclonal, Wuhan, Hubei, China), rabbit anti-β-actin (HRP conjugate, 1:4000; Cell Signaling Technology, Danvers, MA, USA), anti-rabbit IgG (HRP conjugate, 1:2000; Cell Signaling Technology), and anti-mouse IgG (HRP conjugate, 1:2000; Cell Signaling Technology).

Immunohistochemical Staining

Animals were transcardially perfused as the method described above 42 days after the hNSC application. Coronal sections (30 μm) were successively blocked in 0.3% Triton X-100 for 15 min and 2% goat serum for 1 h at room temperature followed by incubation with the primary antibody diluted with blocking buffer at 4°C overnight. Appropriately coupled secondary antibodies were used for single or double labeling for 1 h. After washing, the sections were mounted on glass slides and coverslipped using fluorescence mounting media Dapi Fluoromount-G (Southern Biotech, Birmingham, AL, USA). All secondary antibodies were

tested for cross-reactivity and nonspecific immunoreactivity. For MBP staining, 2–3 fluorescence images were captured from different brain regions in each brain section (illustrated as squares in Figure 3E) with a fluorescence microscope (Olympus, Japan). The fluorescence intensity was measured using ImageJ software (NIH, Bethesda, Maryland, USA). The relative fluorescence intensity of ipsilateral area was calculated using the following equation: $(F_i/F_c) \times 100\%$, where F_i: fluorescence intensity of ipsilateral area and F_c: fluorescence intensity of contralateral area. For quantitative analysis of $HuNu^+/NeuN^+$ and $HuNu^+/GFAP^+$ cell number, six coronal sections at bregma (mm) +1.00, +0.48, −0.26, −2.12, −2.80, and −3.80, respectively, were selected. The following primary and secondary antibodies were used: rabbit anti-NeuN (1:300; Abcam), rabbit antiglial fibrillary acidic protein (GFAP, 1:1000; Dako, Glostrp, Denmark), mouse anti-human nuclei (HuNu, 1:300; Millipore, Billerica, MA, USA), rabbit antimyelin basic protein (MBP, 1:300; Abcam), Alexa Fluor 594 goat anti-mouse IgG (1:1000; Life Technologies, Carlsbad, CA, USA), Alexa Fluor 488 goat anti-rabbit IgG (1:1000; Life Technologies).

Quantification of Brain Tissue Loss

Cryoprotected coronal sections (30 μm) were stained using cresyl violet (CV) staining [15]. We totally selected 10 sections beginning from the bregma 1.70 mm to bregma −4.80 mm with an interval of 540 μm for analysis. The percentage of ipsilateral tissue loss was calculated using the following equation: $(V_c - V_i)/V_c \times 100\%$ [16], where V_c: volume of unlesioned hemisphere and V_i: volume of lesioned hemisphere.

Behavioral Tests

All the behavioral tests were scheduled according to Figure 5A and blindly observed by another examiner. Righting reflex and gait were performed 1, 3, 5, and 7 days after hNSC application as the method described [17]. Grid walking was performed 7 and 14 days after hNSC application on a stainless steel grid plate (40 cm × 80 cm with a mesh size of 4 cm^2), which is elevated 1 m above the floor as the methods described [17,18]. Cognitive neurological function was evaluated using social choice test (SCT) [19,20] within a polyvinyl chloride gray box (60 cm × 90 cm × 40 cm) with removable partitions separating the box into three chambers 28 days after hNSC application. The protocol illustrated in Figure 5E was according to previous method [21]. The whole testing was recorded using digital vidicon (Sony, Tokyo, Japan) and analyzed using an automated tracking software package (Ethovision XT; Noldus Information Technology, Wageningen, the Netherlands) [21]. Preference index was calculated using the following equation: $(d_N - d_F)/(d_N + d_F)$, where d_N: the duration (second) in the chamber containing novel conspecific and d_F: the duration (second) in the chamber containing familiar conspecific. The ability of spatial learning and memory was evaluated 35 days after hNSC application using Morris water maze as the method described [22] within an open circular water-filled pool (120 cm diameter × 50 cm height, temperature at 22 ± 1°C). Animals' swimming behavior was recorded using an overhead video camera connected to an automated tracking software package (Ethovision XT; Noldus Information Technology).

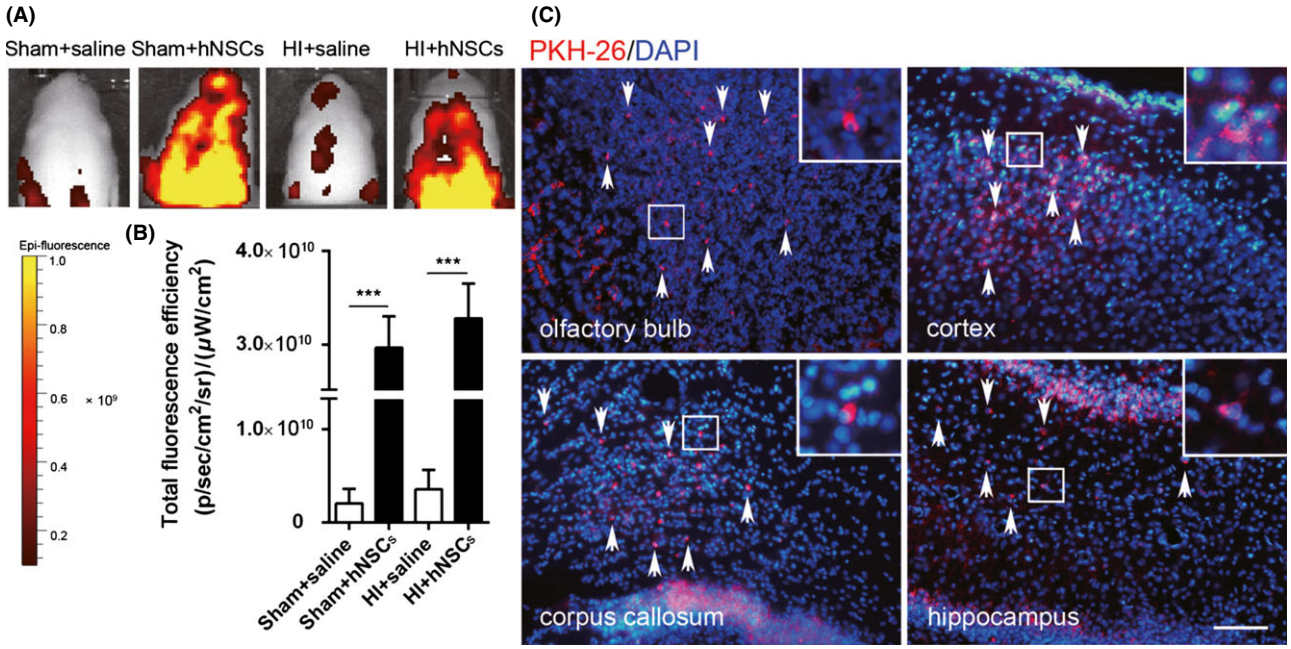

Figure 1 Migration and distribution of human embryonic neural stem cells (hNSCs) after intranasal delivery. (**A**) Representative *in vivo* bioluminescence imaging of the head of P8 SD rat at 3 h after intranasal delivery of PKH-26 (red)-labeled hNSCs (3×10^5 cells/animal). (**B**) Statistical analysis of the total fluorescence efficiency in the brain (n = 3 for each group). ***$P < 0.001$ versus saline-treated group. (**C**) Brain sections of HI + hNSC rats 24 h after intranasal delivery of PKH-26-labeled hNSCs. DAPI (blue) staining was used to demonstrate the nuclei of both host cells and hNSCs. The hNSCs (red, arrows) were found in the area of the olfactory bulb, cortex, corpus callosum, and hippocampus. Scale bar represents 100 μm. HI, hypoxic–ischemic.

Statistical Analysis

Statistical analyses were performed using GraphPad Prism 6.0 (Graph Pad software, San Diego, CA, USA) and Excel software (Microsoft Corporation, Redmond, WA, USA). Values are expressed as mean ± SEM. The data of Western blotting analysis and brain tissue loss of hemisphere were subjected to ordinary one-way analysis of variance (ANOVA) followed by multiple comparisons. Analysis of *in vivo* bioluminescence imaging, righting reflex, gait, grid walking, cumulative duration in each chamber in SCT, data in Morris water maze, and brain tissue loss of sections were performed by two-way ANOVA followed by multiple comparisons. Unpaired two-tailed multiple *t*-test was used for data of preference index in SCT and fluorescence intensity in MBP staining. For all analysis, the changes were considered as statistically significant if the *P*-value was <0.05.

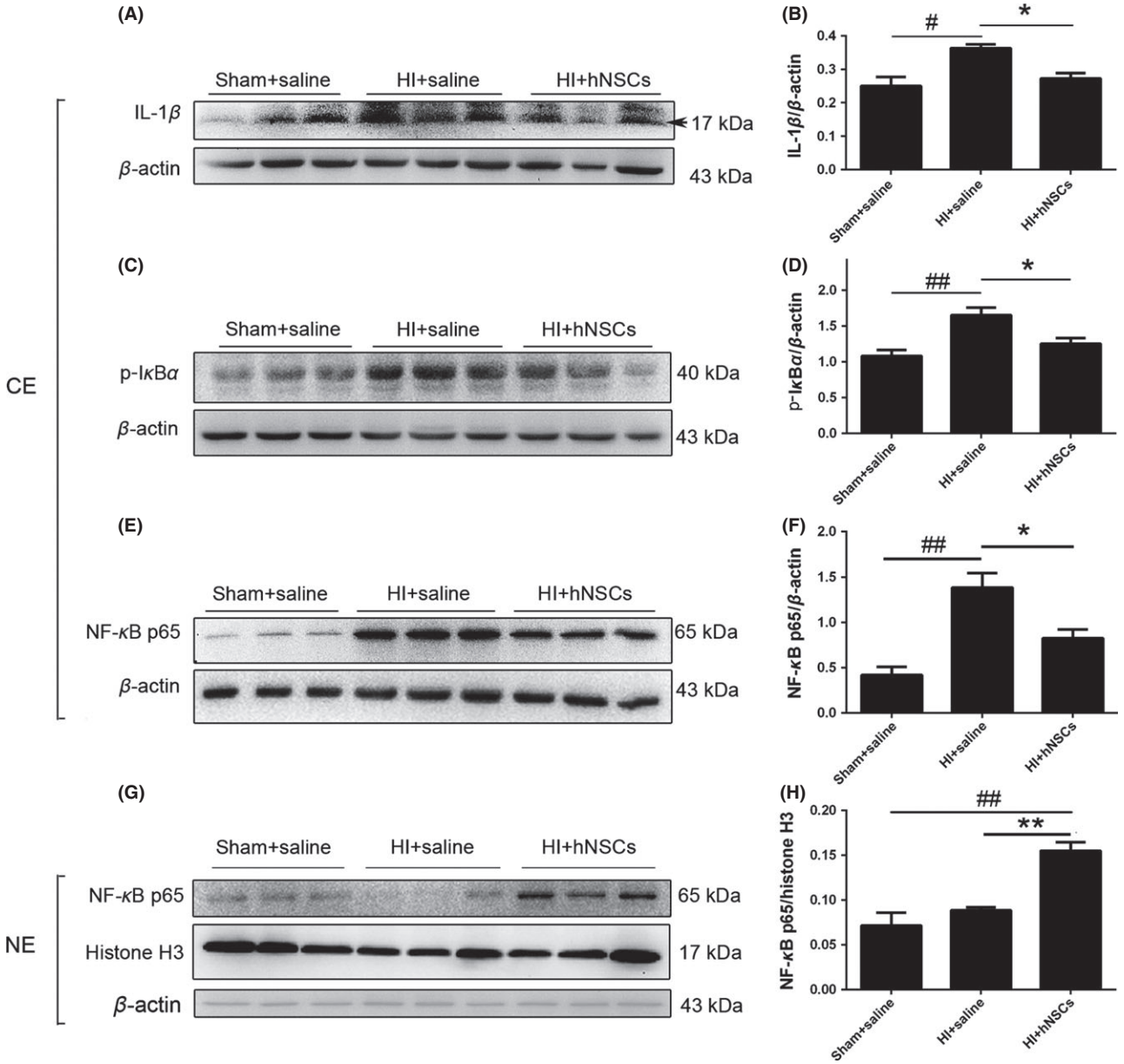

Figure 2 Human embryonic neural stem cells (hNSCs) regulated NF-κB signaling and reduced IL-1β expression. IL-1β, phosphorylated IκBα, and NF-κB p65 expression were detected at day 3 after intranasally delivery using Western blot analysis. **(A**, **C**, **E**, **G)** Representative bands after Western blotting. (**B**, **D**, **F**, **H**) Relative intensities. Hypoxic–ischemic (HI) injury increased cytosolic IL-1β, phosphorylated IκBα, and NF-κB p65 expression, whereas hNSCs reversed the alterations. Note that for nuclear NF-κB, hNSCs significantly enhanced the expression. n = 3 for each group. CE, cytosolic extract; NE, nuclear extract. Arrow indicates the protein molecular weight 17 kDa. $^{*}P < 0.05$, $^{**}P < 0.01$ versus HI + hNSC rats; $^{\#}P < 0.05$, $^{\#\#}P < 0.01$ versus sham + saline rats.

Results

Migration and Distribution of hNSCs After Intranasal Delivery

Migration and distribution of hNSCs after intranasal delivery in the brain was investigated in two separate ways. First, IVIS Lumina XR Imaging system (PerkinElmer) was used to catch the *in vivo* bioluminescence imaging on the heads of neonatal rats at 3 h after intranasal administration (Figure 1A). The efficiency of total PKH-26 fluorescence [(p/second/cm^2/sr)/(μW/cm^2)] in the brain of sham + hNSCs and HI + hNSC rats were much higher than those in the sham + saline and HI + saline rats ($P < 0.001$, Figure 1B). No significant changes were observed between the two hNSC-delivered groups. To further verify the migration and distribution of hNSCs, we observed PKH-26-labeled cells under fluorescence microscopy at 24 h after intranasal delivery. PKH-26-positive cells were detected throughout the layers of the olfactory bulb, cerebral cortex, corpus callosum, and hippocampus in both HI + hNSCs (Figure 1C, arrows) and sham + hNSCs rats (data not shown).

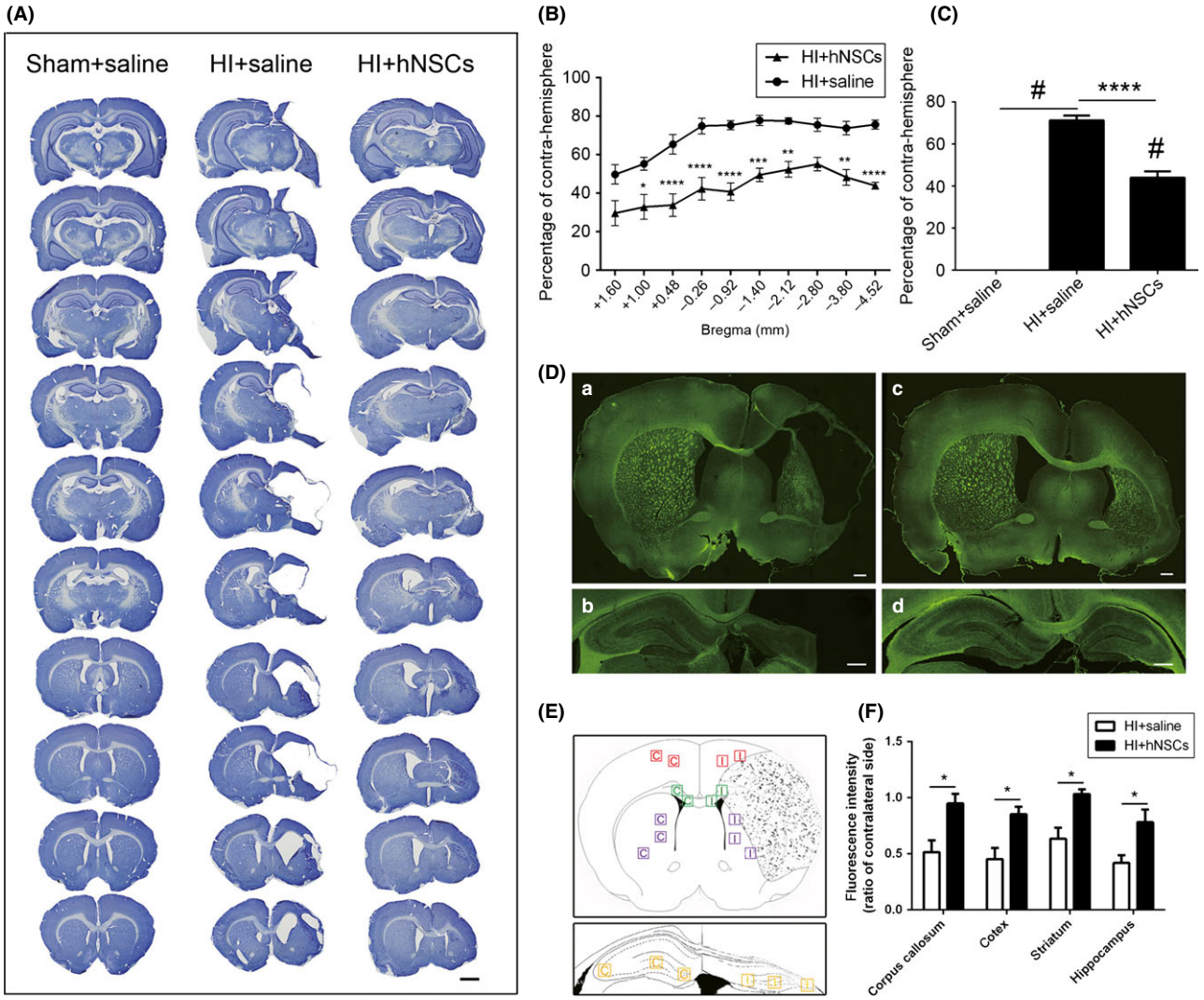

Figure 3 Long-term effects of human embryonic neural stem cells (hNSCs) on brain damage. (**A**) Representative CV- stained sections showing the brain tissue loss 42 days after intranasal delivery. Scale bar represents 2 mm. Percentage of tissue loss in sections (**B**) and ipsi-hemisphere (**C**) were calculated. hNSC application significantly reduced hypoxic–ischemic (HI)-induced tissue loss (n = 5 for HI + saline rats, n = 6 for HI + hNSCs). *$P < 0.05$, **$P < 0.01$, ***$P < 0.001$, ****$P < 0.0001$ versus HI + saline rats; $^{\#}P < 0.0001$ versus sham-operation rats. (**D**) Representative images showing fluorescence intensities of MBP 42 days after intranasal delivery. (**a**, **b**) Sections of HI + saline rats. (**c**, **d**) Sections of HI + hNSC rats. Scale bars represent 600 μm. (**E**) Diagram illustrated the observation areas for each brain region. (**F**) Relative fluorescence intensities in the corpus callosum, cortex, striatum, and hippocampus in HI + saline rats were significantly less than those in HI + hNSC rats (n = 3 for each group). *$P < 0.05$ versus HI + hNSC rats. CV, cresyl violet.

hNSCs Inhibit IL-1β Expression and Promote NF-κB Translocation After HI

We examined the level of cytosolic IL-1β using Western blot analysis at day 3 after intranasal administration. As shown in Figure 2A,B, HI injury significantly upregulated ipsilateral IL-1β level in HI + saline rats ($P < 0.05$ vs. sham + saline rats), whereas hNSC application remarkably reduced IL-1β expression level ($P < 0.05$ vs. HI + saline rats). We also detected phosphorylated IκBα and NF-κB protein expression in the ipsilateral hemisphere 3 days after

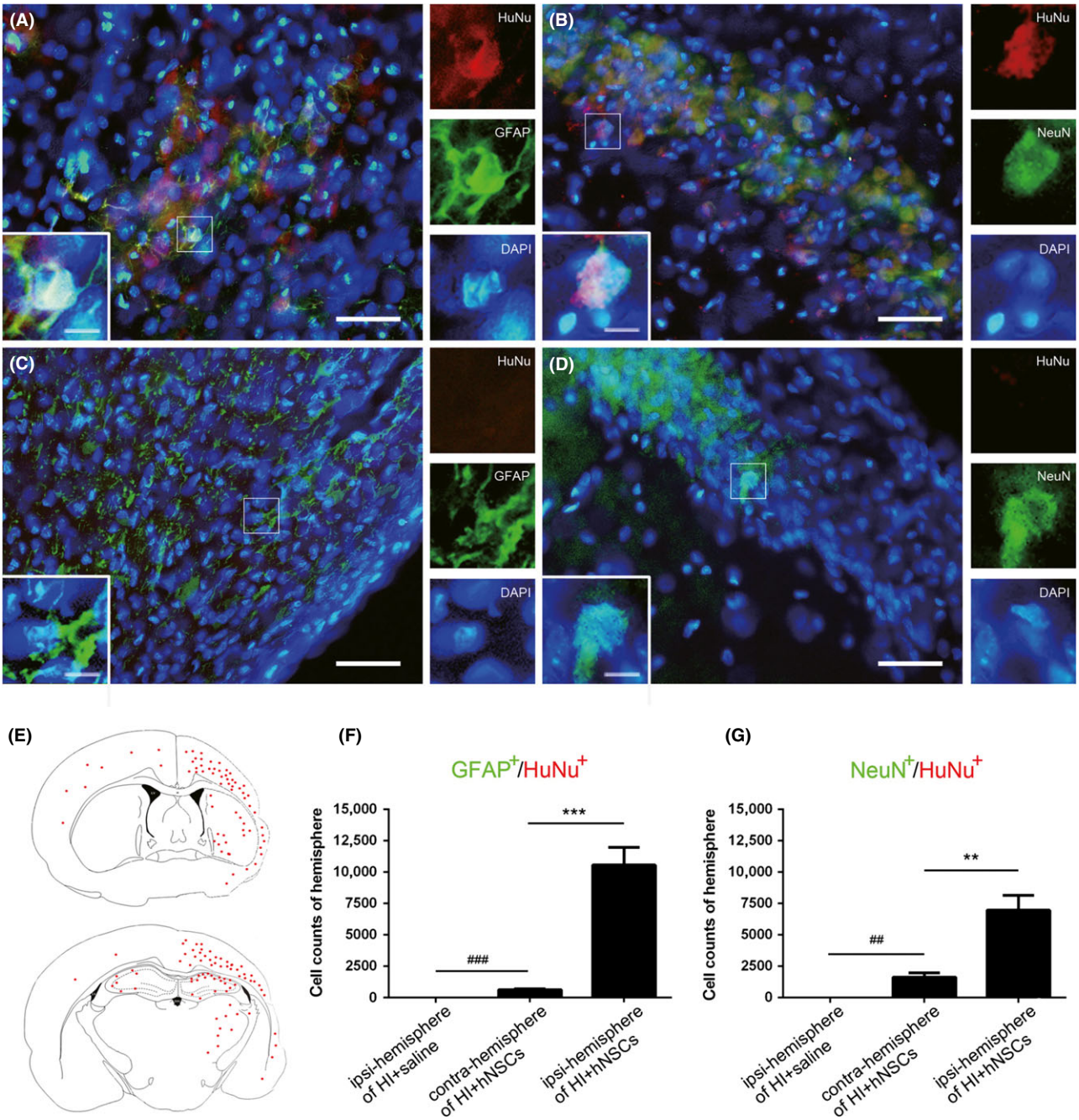

Figure 4 Long-term survival and differentiation of human embryonic neural stem cells (hNSCs) in hypoxic–ischemic (HI) rat brain. (**A**–**D**) Representative immunohistochemically stained brain sections in HI + hNSC rats (**A**, **B**) and in HI + saline rats (**C**, **D**) 42 days after intranasal delivery. Scale bars represent 50 μm (10 μm inset). (**E**) Diagram of distribution of HuNu-positive cells in hNSC-treated HI rats. Note that ipsilateral hemisphere is smaller than contralateral hemisphere because of HI-induced brain tissue loss. Total cell numbers of the GFAP$^+$/HuNu$^+$ (**F**) and NeuN$^+$/HuNu$^+$ (**G**) in ipsilateral or contralateral hemisphere were statistically analyzed. n = 3 for each group. $^{**}P < 0.01$, $^{***}P < 0.001$ versus HI + hNSCs; $^{\#\#}P < 0.01$, $^{\#\#\#}P < 0.001$ versus HI + saline rats.

intranasal administration. As shown in Figure 2C–F, levels of cytosolic Ser32 and Ser36 phosphorylation IκBα and NF-κB p65 were significantly higher in HI + saline rats when compared with those in sham + saline rats ($P < 0.01$). hNSCs notably depressed the HI-induced upregulation in phosphorylated IκBα and NF-κB p65 ($P < 0.05$ vs. HI + saline rats, Figure 2C–F). The content of nuclear NF-κB p65 level was unchanged in HI + saline when compared with sham + saline rats, but significantly increased in HI + hNSC rats ($P < 0.01$ vs. HI + hNSCs, Figure 2G,H).

hNSCs Ameliorate Brain Tissue Loss and White Matter Injury After HI

To quantify long-term effects of hNSCs on brain tissue loss, CV staining was used at day 42 after the hNSC application. As shown in Figure 3A–C, ipsilateral tissue loss was significantly increased in HI + saline rats ($P < 0.0001$ vs. sham + saline rats). hNSC application significantly reduced the percentage of brain tissue loss ($P < 0.0001$ vs. HI + saline rats, Figure 3C) induced by HI. MBP is the specific marker of mature oligodendrocytes. We performed immunohistochemistry to evaluate MBP levels 42 days after hNSC application. As shown in Figure 3D–F, relative fluorescence intensities of MBP in the corpus callosum, cortex, striatum, and hippocampus in HI + saline rats were significantly less than those in HI + hNSC rats ($P < 0.05$).

Long-Term Survival and Differentiation of hNSCs in HI Rat Brain

The long-term survival and differentiation of hNSCs in HI rats was examined 42 days after intranasal delivery. Immunostaining confirmed that the majority of HuNu (a specific marker of human nuclei)-positive cells were observed in ipsi-hemisphere of HI + hNSC rats, and co-existed with NeuN or GFAP (Figure 4A, B). No HuNu-positive cells were seen in HI + saline rats (Figure 4C,D). The distribution region of HuNu-positive cells in the brain of HI + hNSC rats was illustrated in Figure 4E. Moreover, in HI + hNSC rats, $HuNu^+/NeuN^+$ and $HuNu^+/GFAP^+$ cells in the ipsi-hemisphere were significantly more than those in the contra-hemisphere ($P < 0.001$ for $HuNu^+/GFAP^+$ cells, $P < 0.01$ for $HuNu^+/NeuN^+$ cells, Figure 4F,G).

hNSCs Improve Neurological Outcomes After HI

We performed behavioral tests of righting reflex, gait test, grid walking, SCT, Morris water maze following the sequence illustrated in Figure 5A. The sensorimotor function in righting reflex and gait test was impaired after HI. As shown in Figure 5B, at both day 1 and 3 after treatment, HI + hNSC rats spent much less time (second) than HI + saline rats ($P < 0.05$ for day 1, $P < 0.01$ for day 3, respectively) on righting themselves. Meanwhile, HI + hNSC rats moved outside the circular paper faster than HI + saline rats ($P < 0.05$, Figure 5C) at day 5 after intranasal administration. No significant difference was observed between groups of HI + hNSCs and HI + saline at day 7 after hNSC administration, which indicated that sensorimotor impairment after HI injury might be improved in association with the development of neonatal rats. Similar results on sensorimotor functional impairment were observed in grid walking at day 7 after hNSC application. As shown in Figure 5D, the fault ratio in right forelimb significantly increased after HI injury in HI + saline rats and decreased in HI + hNSC rats ($P < 0.05$ vs. HI + saline rats) at day 7 but not day 14 after hNSC delivery. These observed differences were not due to the overall changes in motor activity, because there was no significant difference in the total steps among groups (data not shown).

Rats were tested in the SCT for sociability and social novelty preference following the protocol illustrated in Figure 5E at day 28 after intranasal administration. As shown in Figure 5F, in the acclimation trial, no differences among groups were observed in time spent duration in L and R, which indicated that there is no position preference in all rats. In the sociability trial, sham-operation and HI + hNSC rats prefer to spend much longer time (second) staying in R (C1 contained room) than in L (empty room, $P < 0.001$ vs. R), whereas HI + saline rats did not show the social preference. In the social novelty trial, sham-operation and HI + hNSC rats tended to spend more time in L (novel C2 contained) than in R (nonnovel C1 contained), while the HI + saline rats showed the reverse tendency. To measure recognition of novelty over familiarity, preference index scores were examined. Remarkable decrease in preference index was observed in HI + saline rats when using center point ($P < 0.05$ vs. sham + saline rats) and nose point ($P = 0.0568$ vs. sham + saline rats) for statistical analysis. hNSC treatment reversed these reduction ($P < 0.05$ vs. HI + saline rats, Figure 5G,H).

Morris water maze was performed 35 days after hNSC application to evaluate long-term spatial learning and memory ability. In the acquisition trial (Figure 5I), HI + saline rats showed decreased spatial learning ability with significantly increased escape latency (second) ($P < 0.001$ vs. sham-operation rats) at the training days. HI + hNSC rats showed better learning ability with remarkable

Figure 5 Human embryonic neural stem cells (hNSCs) ameliorated the impairment in sensorimotor, learning, memory, and cognition after hypoxic–ischemic (HI). (**A**) Time schedule for the induction of HI, hNSC application and the time points for various behavioral tests. (**B**, **C**) Performance of righting reflex (**B**) and gait testing (**C**) in groups of sham + saline (n = 23), sham + hNSCs (n = 24), HI + saline (n = 17), and HI + hNSCs (n = 17). (**D**) Performance of grid walking (n = 12 for each group). $^*P < 0.05$, $^{**}P < 0.01$ versus HI + hNSC rats. (**E**–**H**) Performance of social choice test (SCT). (**E**) Experimental testing design of SCT. (**F**) Cumulative time spent in chamber L or R was analyzed for each group. Note that HI + hNSC rats showed consistent preference with sham-operation rats in both sociability and social novelty, whereas HI + saline rats displayed opposite preference in social novelty. HI + hNSC rats, but not HI + saline rats, showed similar preference index of both nose point (**G**) and center point (**H**) with sham-operation rats. n = 12 for each group. L, Left chamber; R, Right chamber. $^{\#}P < 0.05$ versus sham + saline; $^*P < 0.05$ versus HI + saline rats; $^{***}P < 0.001$ for L versus R. (**I**–**K**) Performance of Morris water maze. (**I**) In acquisition trial, HI + saline rats had significantly longer latency than HI + hNSCs and sham-operation rats. In retention trial, both the percentage of time spent in target quadrant (**J**) and frequency across the platform (**K**) was reduced in the HI + saline rats, when compared with sham + saline and HI + hNSC rats. n = 12 for each group. $^*P < 0.05$, $^{**}P < 0.01$, $^{***}P < 0.001$ versus HI + saline; $^{\#}P < 0.001$ versus sham + saline rats.

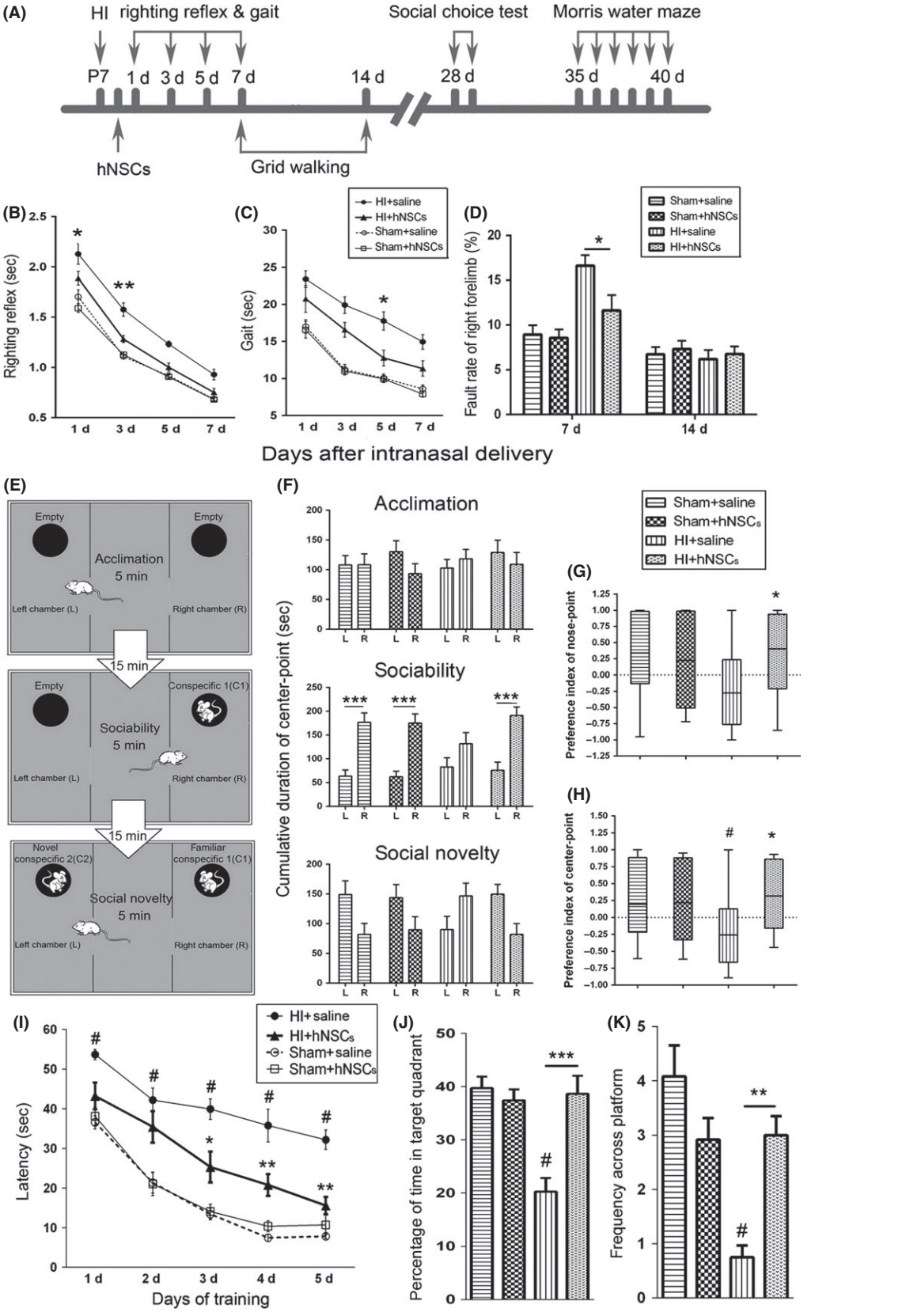
(A)
HI
righting reflex & gait
Social choice test
Morris water maze
P7
1 d
3 d
5 d
7 d
14 d
28 d
35 d
40 d
hNSCs
Grid walking
(B)
Righting reflex (sec)
1 d
3 d
5 d
7 d
(C)
HI+saline
HI+hNSCs
Sham+saline
Sham+hNSCs
Gait (sec)
(D)
Sham+saline
Sham+hNSCs
HI+saline
HI+hNSCs
Fault rate of right forelimb (%)
7 d
14 d
Days after intranasal delivery
(E)
Empty
Empty
Acclimation
5 min
Left chamber (L)
Right chamber (R)
15 min
Empty
Conspecific 1(C1)
Sociability
5 min
15 min
Novel conspecific 2(C2)
Familiar conspecific 1(C1)
Social novelty
5 min
(F)
Acclimation
Sociability
Social novelty
Cumulative duration of center-point (sec)
L
R
(G)
Sham+saline
Sham+hNSCs
HI+saline
HI+hNSCs
Preference index of nose-point
(H)
Preference index of center-point
(I)
HI+saline
HI+hNSCs
Sham+saline
Sham+hNSCs
Latency (sec)
1 d
2 d
3 d
4 d
5 d
Days of training
(J)
Percentage of time in target quadrant
(K)
Frequency across platform

reduction in escape latency at the 3rd, 4th and 5th day of training when compared with HI + saline rats ($P < 0.05$ for the 3rd day, $P < 0.01$ for the 4th and 5th day). There was no statistically significant difference among groups in swimming time and distance (data not shown). In the retention trial, significant reduction in the percentage of time spent in the target quadrant ($P < 0.01$) and frequency across the platform ($P < 0.001$) were observed in HI + saline rats, when compared with HI + hNSC rats (Figure 5J, K).

Discussion

Among cell therapy studies, intranasal delivery has been reported to be noninvasive and relatively safe in comparison with invasive intracranial transplantation [23,24]. In the present study, we intranasally delivered 3×10^5 hNSCs and found that these fluorescence-labeled cells could rapidly bypass the blood–brain barrier, migrate and distribute into extensive brain regions in both hemisphere. The migration routes are possibly from nasal mucosa through cribriform plate along olfactory neural pathway into brain regions and cerebrospinal fluid [25]. The dosage and administration time we used are according to our previous work and others [26,27]. These results further confirmed the applicability of intranasal delivery and support the notion that hNSCs have the homing instinct toward the CNS [25].

Previous studies showed that HI injury induces rapid activation in microglia and astrocyte, which then produce various pro-inflammatory cytokines [6,28]. In the present study, IL-1β expression level increased after HI injury, indicating that neuroinflammatory responses are activated. In agreement with the study described in a rat stroke model [29], we observed a remarkable reduction in IL-1β level 3 days after hNSC treatment. Our findings suggest that hNSC application could modulate the immune response in the CNS and thus protecting the neurons and glial cells against inflammatory injury.

Transcriptional factor NF-κB functions in both protective and damaging pathways during brain injury [30]. Studies found that IκBα plays important roles in regulating NF-κB signaling via mediating cytosolic-nuclear translocation of NF-κB [31]. In this study, we found a coincident upregulation in cytoplasmic NF-κB p65 and phosphorylated IκBα protein expression 4 days after HI occurred, and remarkable repression 3 days after hNSC treatment. These results could be supported by previous work because reduction in cytosolic phosphorylated IκBα and NF-κB results in strong neuroprotection against HI injury [30,32].

Despite the significant increase in cytosolic NF-κB p65 and phosphorylated IκBα expression, we did not find any changes in nuclear NF-κB p65 level after HI. Our results differ from previous study, which reported that nuclear NF-κB p65 level upregulates within 3 h after HI [32]. This discrepancy might due to the different observation time points because we detected p65 levels at day 4 after HI injury. Previous studies have demonstrated that during persistent stimulation, cytosolic IκBα can enter into the nucleus, help removing NF-κB p65/p50 dimers from DNA binding site, and backing to the cytosol, thus decrease nuclear NF-κB level [33–36]. In the present study, we suppose that at day 4 after HI, the persistent stimulation from HI-induced biochemical cascades triggers this feedback regulation and limits nuclear NF-κB localization. Further researches are needed to evaluate how the dynamic changes in cytosolic-nuclear NF-κB/IκBα translocation are modulated during the process of HI-induced brain injury. Interestingly, in our study, we observed a remarkable increase in nuclear NF-κB p65 level in hNSC-treated rats, which suggested that hNSCs could maintain the NF-κB signaling at day 4 after HI injury. The enhanced nuclear NF-κB p65 expression is possibly related to the hNSC-induced suppression on NF-κB feedback regulation, as hNSCs have been proved to reduce neuroinflammation in our and other's work [29]. hNSC-induced nuclear NF-κB signaling upregulation might be protective in neurofunctional recovery of HI rats. Such speculation could be supported by previous studies, as hNSCs have been demonstrated to promote neural circuit remolding via synaptic reconstruction [26,37,38], and several studies have also reported that NF-κB plays important roles in synaptic signaling modulation, learning/memory, and cognition [39–41]. Therefore, these results indicate that hNSCs may improve neural plasticity via upregulating NF-κB signaling.

Our previous work found that hNSC transplantation improves sensorimotor outcomes in a middle cerebral artery occlusion rat model [27]. In the present study, we further confirmed that hNSCs promote neurobehavioral recovery against HI injury in both sensorimotor ability and long-term learning, memory, and cognition. Exogenous hNSCs maintained survival and differentiated into both neurons and astrocytes in lesioned area even at the last observation day (42 days after hNSC application), which was possibly due to the pro-survival effect of enhanced growth factors/trophic factors in lesion area [42]. Therefore, our results indicated that hNSCs may repair brain injury through cell replacement in HI rats.

In conclusion, our results found that hNSC treatment significantly reduced brain tissue loss and white matter injury, ameliorated sensorimotor disabilities, and improved learning, memory, and cognitive deficits after HI. Additionally, we provided the first evidence that hNSCs could promote NF-κB translocation and downregulate the expression of IL-1β 3 days after intranasal delivery in neonatal HI rats. These findings demonstrated that intranasal delivery of hNSCs 24 h after HI resulted in both early and long-term protective effects, which possibly involves the molecular modulation of NF-κB signaling.

Acknowledgment

We thank Ms. Qian-Ying Huang for her kindly help performing social choice test. This work was supported by grants from the Shanghai Municipality, China (No. 13431901203), National Natural Scientific Foundation, China (81170322), Shanghai Natural Scientific Foundation, China (11ZR1405300), and Shanghai Municipal Outstanding Talent Development Foundation (2012052).

Conflict of Interest

The authors declare no conflict of interest.

References

1. Iwai M, Cao G, Yin W, Stetler RA, Liu J, Chen J. Erythropoietin promotes neuronal replacement through revascularization and neurogenesis after neonatal hypoxia/ischemia in rats. *Stroke* 2007;**38**:2795–2803.
2. Tata DA, Markostamou I, Ioannidis A, et al. Effects of maternal separation on behavior and brain damage in adult rats exposed to neonatal hypoxia-ischemia. *Behav Brain Res* 2015;**280**:51–61.
3. Mwaniki MK, Atieno M, Lawn JE, Newton CR. Long-term neurodevelopmental outcomes after intrauterine and neonatal insults: A systematic review. *Lancet* 2012;**379**:445–452.
4. Shankaran S, Pappas A, McDonald SA, et al. Childhood outcomes after hypothermia for neonatal encephalopathy. *N Engl J Med* 2012;**366**:2085–2092.
5. Azevedo-Pereira RL, Medei E, Mendez-Otero R, Souza JP, Alves-Leon SV. Isolation of neurosphere-like bodies from an adult patient with refractory temporal lobe epilepsy. *Arq Neuropsiquiatr* 2010;**68**:956–958.
6. Thornton C, Rousset CI, Kichev A, et al. Molecular mechanisms of neonatal brain injury. *Neurol Res Int* 2012;**2012**:506320.
7. Mattson MP, Goodman Y, Luo H, Fu W, Furukawa K. Activation of NF-kappaB protects hippocampal neurons against oxidative stress-induced apoptosis: Evidence for induction of manganese superoxide dismutase and suppression of peroxynitrite production and protein tyrosine nitration. *J Neurosci Res* 1997;**49**:681–697.
8. Tamatani M, Che YH, Matsuzaki H, et al. Tumor necrosis factor induces Bcl-2 and Bcl-x expression through NFkappaB activation in primary hippocampal neurons. *J Biol Chem* 1999;**274**:8531–8538.
9. Limtrakul P, Yodkeeree S, Pitchakarn P, Punfa W. Suppression of inflammatory responses by black rice extract in RAW 264.7 macrophage cells via downregulation of NF-κB and AP-1 signaling pathways. *Asian Pac J Cancer Prev* 2015;**16**:4277–4283.
10. Merlo E, Freudenthal R, Maldonado H, Romano A. Activation of the transcription factor NF-kappaB by retrieval is required for long-term memory reconsolidation. *Learn Mem* 2005;**12**:23–29.
11. Wallace PK, Tario JD Jr, Fisher JL, Wallace SS, Ernstoff MS, Muirhead KA. Tracking antigen-driven responses by flow cytometry: Monitoring proliferation by dye dilution. *Cytometry Part A* 2008;**73**:1019–1034.
12. Rice JE, Vannucci RC, Brierley JB. The influence of immaturity on hypoxic-ischemic brain damage in the rat. *Ann Neurol* 1981;**9**:131–141.
13. Ross TM, Martinez PM, Renner JC, Thorne RG, Hanson LR, Frey WH. Intranasal administration of interferon beta bypasses the blood–brain barrier to target the central nervous system and cervical lymph nodes: A non-invasive treatment strategy for multiple sclerosis. *J Neuroimmunol* 2004;**151**:66–77.
14. Wang C, Yang F, Liu X, Liu M, Zheng Y, Guo J. Neurotrophic signaling factors in brain ischemia/reperfusion rats: Differential modulation pattern between single-time and multiple electroacupuncture stimulation. *Evid Based Complement Alternat Med* 2014;**2014**:625050.
15. Swanson RA, Morton MT, Tsao-Wu G, Savalos RA, Davidson C, Sharp FR. A semiautomated method for measuring brain infarct volume. *J Cerebr Blood F Met* 1990;**10**:290–293.
16. Yin W, Cao G, Johnnides MJ, et al. TAT-mediated delivery of Bcl-xL protein is neuroprotective against neonatal hypoxic-ischemic brain injury via inhibition of caspases and AIF. *Neurobiol Dis* 2006;**21**:358–371.
17. Lubics A, Reglodi D, Tamas A, et al. Neurological reflexes and early motor behavior in rats subjected to neonatal hypoxic-ischemic injury. *Behav Brain Res* 2005;**157**:157–165.
18. Rogers DC, Campbell CA, Stretton JL, Mackay KB. Correlation between motor impairment and infarct volume after permanent and transient middle cerebral artery occlusion in the rat. *Stroke* 1997;**28**:2060–2065.
19. Nadler JJ, Moy SS, Dold G, et al. Automated apparatus for quantitation of social approach behaviors in mice. *Genes Brain Behav* 2004;**3**:303–314.
20. Vetter-O'Hagen CS, Spear LP. The effects of gonadectomy on sex- and age-typical responses to novelty and ethanol-induced social inhibition in adult male and female Sprague–Dawley rats. *Behav Brain Res* 2012;**227**:224–232.
21. Eagle AL, Fitzpatrick CJ, Perrine SA. Single prolonged stress impairs social and object novelty recognition in rats. *Behav Brain Res* 2013;**256**:591–597.
22. Chen W, Ma Q, Suzuki H, Hartman R, Tang J, Zhang JH. Osteopontin reduced hypoxia-ischemia neonatal brain injury by suppression of apoptosis in a rat pup model. *Stroke* 2011;**42**:764–769.
23. Danielyan L, Schafer R, von Ameln-Mayerhofer A, et al. Intranasal delivery of cells to the brain. *Eur J Cell Biol* 2009;**88**:315–324.
24. Donega V, Nijboer CH, van Tilborg G, Dijkhuizen RM, Kavelaars A, Heijnen CJ. Intranasally administered mesenchymal stem cells promote a regenerative niche for repair of neonatal ischemic brain injury. *Exp Neurol* 2014;**261**:53–64.
25. Ding DC, Lin CH, Shyu WC, Lin SZ. Neural stem cells and stroke. *Cell Transplant* 2013;**22**:619–630.
26. Daadi MM, Davis AS, Arac A, et al. Human neural stem cell grafts modify microglial response and enhance axonal sprouting in neonatal hypoxic-ischemic brain injury. *Stroke* 2010;**41**:516–523.
27. Liu XY, Wang CP, Liu M, Ji G, Guo JC. Transplantation of human embryonic neural stem cells protects rats against cerebral ischemic injury. *Sheng Li Xue Bao* 2014;**66**:691–701.
28. Inder TE, Volpe JJ. Mechanisms of perinatal brain injury. *Semin Neonatol* 2000;**5**:3–16.
29. Huang L, Wong S, Snyder EY, Hamblin MH, Lee J-P. hNSCs ameliorate inflammation in early-stage ischemic injury. *Stem Cell Res Ther* 2014;**5**:129.
30. Kaltschmidt B, Kaltschmidt C. NF-kappaB in the nervous system. *Cold Spring Harb Perspect Biol* 2009;**1**:a001271.
31. Place RF, Haspeslagh D, Hubbard AK, Giardina C. Cytokine-induced stabilization of newly synthesized I (kappa)B-alpha. *Biochem Biophys Res Commun* 2001;**283**:813–820.
32. Nijboer CH, Heijnen CJ, Groenendaal F, May MJ, van Bel F, Kavelaars A. Strong neuroprotection by inhibition of NF-kappaB after neonatal hypoxia-ischemia involves apoptotic mechanisms but is independent of cytokines. *Stroke* 2008;**39**:2129–2137.
33. Arenzana-Seisdedos F, Thompson J, Rodriguez MS, Bachelerie F, Thomas D, Hay RT. Inducible nuclear expression of newly synthesized I kappa B alpha negatively regulates DNA-binding and transcriptional activities of NF-kappa B. *Mol Cell Biol* 1995;**15**:2689–2696.
34. Bachelerie F, Rodriguez MS, Dargemont C, et al. Nuclear export signal of IkappaBalpha interferes with the Rev-dependent posttranscriptional regulation of human immunodeficiency virus type I. *J Cell Sci* 1997;**110**:2883–2893.
35. Arenzana-Seisdedos F, Turpin P, Rodriguez M, et al. Nuclear localization of I kappa B alpha promotes active transport of NF-kappa B from the nucleus to the cytoplasm. *J Cell Sci* 1997;**110**:369–378.
36. Rodriguez MS, Thompson J, Hay RT, Dargemont C. Nuclear retention of IkappaBalpha protects it from signal-induced degradation and inhibits nuclear factor kappaB transcriptional activation. *J Biol Chem* 1999;**274**:9108–9115.
37. Daadi MM, Steinberg GK. Manufacturing neurons from human embryonic stem cells: Biological and regulatory aspects to develop a safe cellular product for stroke cell therapy. *Regen Med* 2009;**4**:251–263.
38. Armstrong RJ, Hurelbrink CB, Tyers P, et al. The potential for circuit reconstruction by expanded neural precursor cells explored through porcine xenografts in a rat model of Parkinson's disease. *Exp Neurol* 2002;**175**:98–111.
39. Kassed CA, Herkenham M. NF-kappaB p50-deficient mice show reduced anxiety-like behaviors in tests of exploratory drive and anxiety. *Behav Brain Res* 2004;**154**:577–584.
40. Meffert MK, Chang JM, Wiltgen BJ, Fanselow MS, Baltimore D. NF-kappa B functions in synaptic signaling and behavior. *Nat Neurosci* 2003;**6**:1072–1078.
41. Salles A, Romano A, Freudenthal R. Synaptic NF-kappa B pathway in neuronal plasticity and memory. *J Physiol Paris* 2014;**108**:256–262.
42. Bejot Y, Prigent-Tessier A, Cachia C, et al. Time-dependent contribution of non neuronal cells to BDNF production after ischemic stroke in rats. *Neurochem Int* 2011;**58**:102–111.

Supporting Information

The following supplementary material is available for this article:

Appendix S1 Structural diagram of social choice test apparatus.

Appendix S2 The expression of nuclear p-IκBα levels in all the groups 3 days after intranasal delivery.